Journal of Manufacturing Processes 61 (2021) 1–14

Contents lists available at ScienceDirect

Journal of Manufacturing Processes

journal homepage: www.elsevier.com/locate/manpro

Surface modification of ultrahigh strength 300M steel under supercritical carbon dioxide ($scCO_2$)-assisted grinding process

Jiaqiang Dang [a,b], Heng Zhang [a,b], Qinglong An [a,b,*], Weiwei Ming [a,b], Ming Chen [a,b]

[a] State Key Laboratory of Mechanical Systems and Vibration, Shanghai Jiao Tong University, Shanghai, 200240, China
[b] School of Mechanical Engineering, Shanghai Jiao Tong University, Shanghai, 200240, China

ARTICLE INFO

Keywords:
300M steel
Supercritical carbon dioxide
Grinding
Surface modification

ABSTRACT

300M steel has been widely utilized in the manufacturing processes of functional parts served in harsh environments. The properties of the parts' surface layer induced by the grinding process are of great importance for the service performance, which can be determined by the input parameters of processing. This paper carried out evaluation of surface modification of 300M steel material under the $scCO_2$-assisted grinding process. To further enhance the understanding of this processing design, the generation of surface modification with dry and flood techniques were also compared. The surface morphology, surface roughness, microstructure evolution, work hardening and surface residual stresses were recorded. The mechanism of grain refinement and the substructure of the martensite lath has been revealed. It was found that the $scCO_2$-assisted grinding processes are responsible for smoother surface profile compared to the dry and flood techniques. Meanwhile, the machined surface roughness was maintained at a stable lower level as the grinding depth increases, proving the great superiority of $scCO_2$ medium for improving the productivity and process sustainability. The grains in the superficial layer have been noticeably refined after grinding operation while it presents deeper refinement with $scCO_2$-assisted grinding process. Meanwhile, nanocrystalline and carbide precipitation were clearly found on the refined layer with $scCO_2$ medium, the crystal defects are mainly the combination of dislocation tangles (DTs), dislocation walls (DWs) and dislocation cells (DCs), and the stacking fault was observed to be the substructure for the lath martensite except the dislocation with TEM analysis. The designed $scCO_2$-assisted grinding contributes to higher work hardening and compressive stresses compared to dry and flood methods.

Introduction

In comparison to common steels, 300 M characterized as a low alloy and ultrahigh strength steel has been increasingly utilized in the manufacture of aircraft landing gears and structural parts such as fasteners, pressure vessels and aerospace gears owing to its superior mechanical properties [1]. Grinding is one of the most important and final manufacturing processes in the industry for making the aforementioned components. High dimensional precision and superior surface finish are demanded outputs of this process for ground components by using abrasive wheels [2,3]. As reported by Li et al. [4], in grinding process machined surface is created by a number of grains with negative rake angle under the grinding input parameters. Surface quality is influenced by wheel constituents, grit size, input parameters and cooling conditions. Meanwhile, grinding generates greater energy consumption for removing the identical workpiece material than that of other conventional machining processes due to the cutting responses of numerous tool edges [5]. On the basis of grinding depths and kinematics a single grit may experience elastic sliding, plastic ploughing and cutting actions [6,7]. All of these actions lead a high specific energy into surface grinding process [8]. The heat generated on the machined zone is delivered by the grinding wheel, workpiece, coolants and chips, and thermal damage of machined surface is the focus of grinding process [9]. Therefore, the application of coolants and lubricants is necessary to dissipate the heat, especially the heat distributed over the workpiece to optimize the machined surface quality [10,11].

Conventionally liquid coolants are used in grinding process. However, these flood systems also bring several economic, environmental and biological disadvantages to the global community. Moreover, the liquid is hard to penetrate into the cutting area since the excessively high temperatures usually lead to the premature rupture of lubricant film in flood cooling, resulting in poor permeability and reduction of cooling

* Corresponding author at: State Key Laboratory of Mechanical Systems and Vibration, Shanghai Jiao Tong University, Shanghai, 200240, China.
E-mail address: qlan@sjtu.edu.cn (Q. An).

https://doi.org/10.1016/j.jmapro.2020.11.001
Received 11 September 2020; Received in revised form 23 October 2020; Accepted 1 November 2020
Available online 14 November 2020
1526-6125/© 2020 The Society of Manufacturing Engineers. Published by Elsevier Ltd. All rights reserved.

effect [12]. In recent years, the notion of sustainable manufacturing has become crucial within the whole international community to achieve a global development [13]. In the manufacturing process this commonly means green cooling and lubricant methods [14]. Techniques like dry processing, minimum quantity lubrication (MQL) and cryogenic cooling were then developed [15,16]. No doubt that the complete dry condition during grinding eliminates the concerns of contamination and waste disposal. Tawakoli et al. [17] investigated the performance of dry grinding and they concluded that the generated heat can be greatly reduced under special condition during processing. Despite the reduction of environmental concerns dry grinding without any coolants still faces several problems such as wheel wear, adverse metallurgical alternations and burn risks associated with the high generated heat [18]. Therefore, Hermann et al. [19] stated that attention should at least be paid to the study of alternative coolants/lubricants with minimum environmental damage.

An alternative to dry processing can be described in MQL, cryogenic cooling and/or their combination (*i.e.* CMQL). In the case of MQL, it is the least costly technique in comparison to other cooling methods and has both cooling and lubrication effects with a very low fluid usage. As reported by Li et al. [20], the high pressure gas in MQL contributes to the cooling of machining zone and chip removal. Research experiences have also unfolded the way to the use of cryogenic methods to the machining process. Reddy et al. [21] described that application of liquid nitrogen (LN_2) contributed to the elevation of grinding ratio but adversely leads to relatively higher power consumption than dry and conventional oil techniques. However, the installation of the cooling equipment and liquid nitrogen are generally costly and complex. Therefore, according to Teicher et al. [22] the sole use of cryogenic cooling is mostly restricted to very sensitive components which undergo extreme fatigue and dynamic loads for economic reasons. Lin et al. [23] studied the cooling effects of the mentioned methods for titanium alloys. They found that the use of cryogenic minimum quantity lubrication (CMQL) presents optimization on the machined surface integrity in view of lower surface roughness and wear rate than dry and flood cutting conditions.

From the literature survey it is clear that different cooling methods may produce disparate effects on the machined surface. However, the studies regarding the influences of external cooling medium on the surface properties of machined sample are still rare. To shrink the gap, the supercritical carbon dioxide ($scCO_2$) medium was creatively utilized to assist the surface grinding process, in which the effect of cooling medium on the surface modification was specially addressed. Furthermore, a newly developed cooling condition that combined the $scCO_2$ and oil on water (Oow) system (*i.e.* hybrid $scCO_2$-OoW) was also tentatively engaged. The use of this efficient alternative may lead to lower costs in economic view and enrich the scientific field of this topic since comprehensive characterization of 300 M steel material under this cooling method is very limited. In this work, the abrasive grains were protected from wear and efficient refrigeration due to the cryogenic gas was possibly gained. Current work also considered dry and flood techniques as the control group. A variety of topics including surface morphology, microstructure evolution, work hardening and residual stresses were carefully recorded and characterized under different designed ways.

Experimental procedures

Workpiece material

The workpiece material tested in the present work was 300 M ultrahigh strength steel which was machined into cuboid-shaped specimens with a size of 30 (L) × 20 (W) × 15 (H) mm^3. The chemical compositions (*wt.* %) and main mechanical properties of the material are shown in Tables 1 and 2, respectively. It can be noted that the 300 M steel presents considerably higher yield strength (~1600 MPa) and tensile strength (~2000 MPa) while lower elongation (12 %) at fracture than the conventional stainless steel ($\sigma_{s:}$ ~200 MPa, $\sigma_{b:}$ ~500 MPa, ε: 40 %) [24]. Before machining, the samples were cut by wire electrical discharge machining, and then hot mounted, mechanically polished with silicon carbide (SiC) sandpapers ($180^{\#}$, $360^{\#}$, $800^{\#}$, $1200^{\#}$) and a diamond suspension (9 μm, 3 μm and 50 nm), and finally etched with 4% Nital for optical microscope (OM) and scanning electron microscope (SEM) analysis. After that, the sample was used for vibration polishing with a SiO_2 suspension (30 nm) for electron backscattered diffraction (EBSD) observations.

Table 1
Chemical compositions of the 300 M steel workpiece.

Element	C	Si	V	Cr	Mn	Ni	Mo	Fe
wt. %	0.42	1.70	0.08	0.82	0.85	1.86	0.41	Bal.

Table 2
Main mechanical properties of the 300 M steel workpiece.

Workpiece	Yield strength, σ_s (MPa)	Tensile strength, σ_b (MPa)	Elongation, ε (%)	Section shrinkage, δ (%)
300 M steel	1644	1994	12	41

Fig. 1 exhibits the SEM, OM images, inverse pole figure of EBSD and the grain size distribution for the matrix 300 M steel. Note that the main microstructure of the 300 M workpiece was found to be tempered lath martensite and slight bainite, and the average grain size is about 3.1 μm, which was analyzed by the Channel5 software of EBSD data. Besides, the used 300 M steel possessed great strength and hardness in terms of its material constituent.

Cooling methods description

Schematic diagram of the $scCO_2$-based cooling generator is exhibited in Fig. 2. In the process, three separate reservoirs loaded up with liquid carbon dioxide, oil and water are included in the cooling system, and the air compressor was used to provide the power for atomization. The supercritical dioxide ($scCO_2$) is obtained by covering a series of processes including pressuring, heating, atomization and spraying out, and its pressure and temperature maintained at a minimum value of 72.8 atm and 31.2 °C, respectively. The oil and water are conveyed to the mixing container by its individual pump, then atomized through the air jet with high pressure and speed with the air compressor, and finally entered the nozzle. As the associated cooling medium including OoW droplets, heated and pressured CO_2, compressed air meets together in the mixing chamber, their mixture characterized as a cryogenic jet composed of $scCO_2$ and OoW droplets was formed at the nozzle under the Joule-Thomson effect, with a temperature of approximate −78 °C [25]. The mixture finally penetrates into the machining zone and wheel surface with a high speed to significantly reduce the temperature and friction for cryogenic cooling and lubrication. Different cooling methods (*i.e.* $scCO_2$ and $scCO_2$-OoW) can be gained by controlling the flow valves (see Fig. 2) and the diameter of the droplet particles is at the range of 100 ~200 μm, which was measured by the high-speed camera. The details of the cooling methods are listed in Table 3.

Grinding tests

The surface grinding experiments under different cooling conditions were carried out on an MKL 7132 grinder. A conventional zirconium corundum wheel manufactured by Norton Co. was utilized. The cooling and lubrication system were arranged as the experimental setup shown in Fig. 3 (a). The individual $scCO_2$ droplets and the mixture of $scCO_2$ and OoW droplets were sprayed out through two copper nozzles (see the

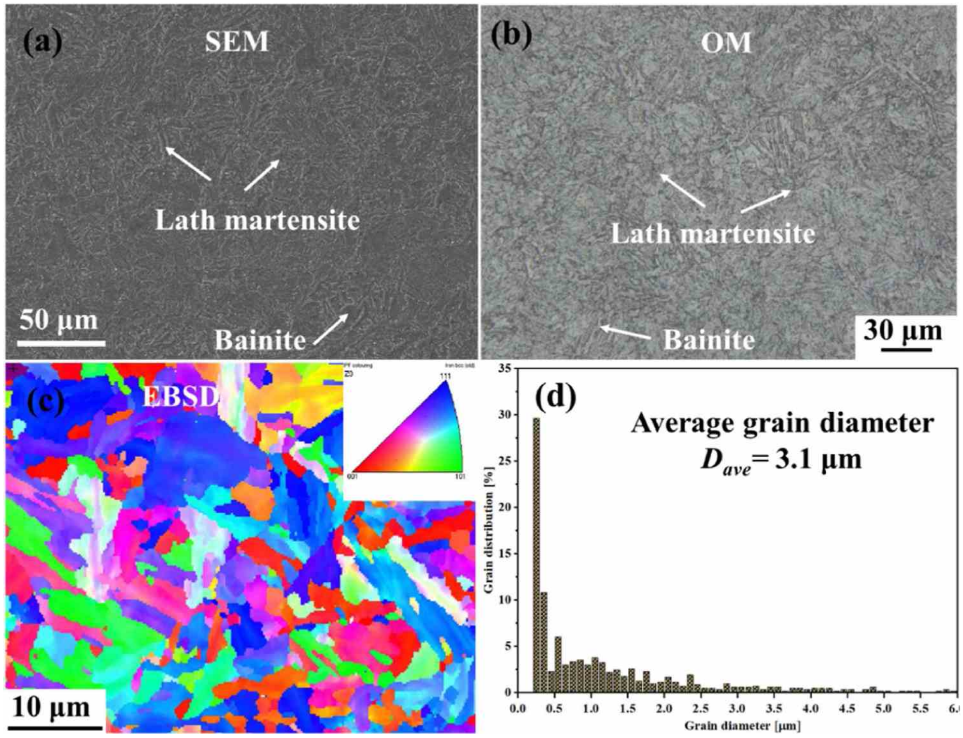

Fig. 1. Sample of 300 M steel: (a) SEM image, (b) OM image, (c) inverse pole figure of EBSD and (d) grain size distribution.

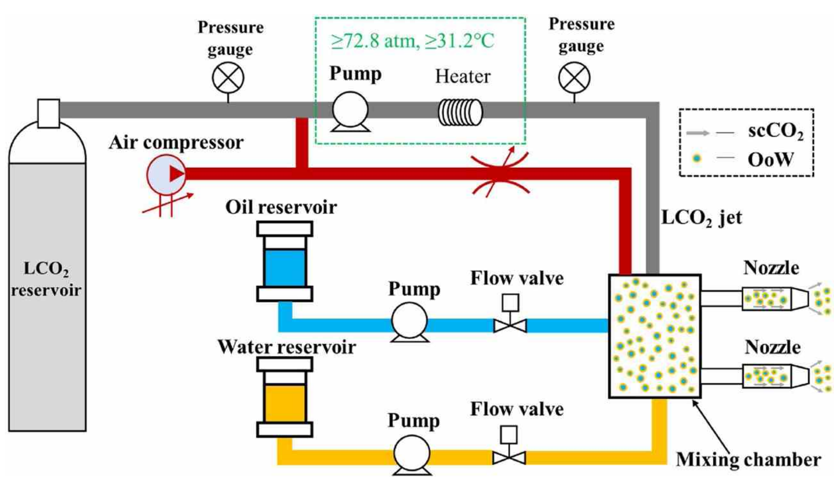

Fig. 2. Schematic diagram of cooling and lubrication system.

Table 3
Cooling methods and their parameters.

Cooling and lubrication methods	Parameters
flood	Grinding fluid: vasco 7000, pressure: 8 bar, flow rate: 120 L/min
$scCO_2$	Grinding fluid: liquid carbon dioxide, pressure: 7.5 bar, flow rate: 50 mL/h
$scCO_2$+OoW	Grinding fluid: liquid carbon dioxide + antifreeze water and soluble vegetable oil (1:1), pressure: 7.5 bar, flow rate: 50 mL/h

yellow arrow) and the grinding fluids was directed into the machining zone through the flood nozzle (see the blue arrow). The mechanism of $scCO_2$ based cooling system was indicated in Fig. 3 (b), in which a film filled with frozen oil and water was formed on the surface of abrasive grain. This contributes to the reduction of friction between the abrasive grains and the workpiece. On the other hand, it may also lead to a certain wheel clogging due to the ductile and viscous chips under wet work environment. Fig. 3 (c) and (d) plot the optical images of abrasive grains and schematic diagram of OoW droplets, respectively. The reservoir of liquid CO_2 and hybrid $scCO_2$-OoW cooling system are shown in Fig. 3 (e).

The conditions of grinding experiments were wheel speed of 20 m/s, feed rate of 100 mm/min, effective grinding depth of 0.025, 0.050, 0.075, and 0.100 mm, respectively. It should be noted that the aforementioned parameters and wheel type were selected based on the industrial manufacture of finish grinding operations, as presented in Table 4. According to the workpiece size and parameters, the specific material removal rate (MRR) was calculated as 1.25, 2.5, 3.75, 5 mm^3/s following the equation of MRR $= \frac{v_w \cdot L \cdot a_p}{60}$, respectively. The grinding wheel was trimming using the diamond wheel dresser after each test to

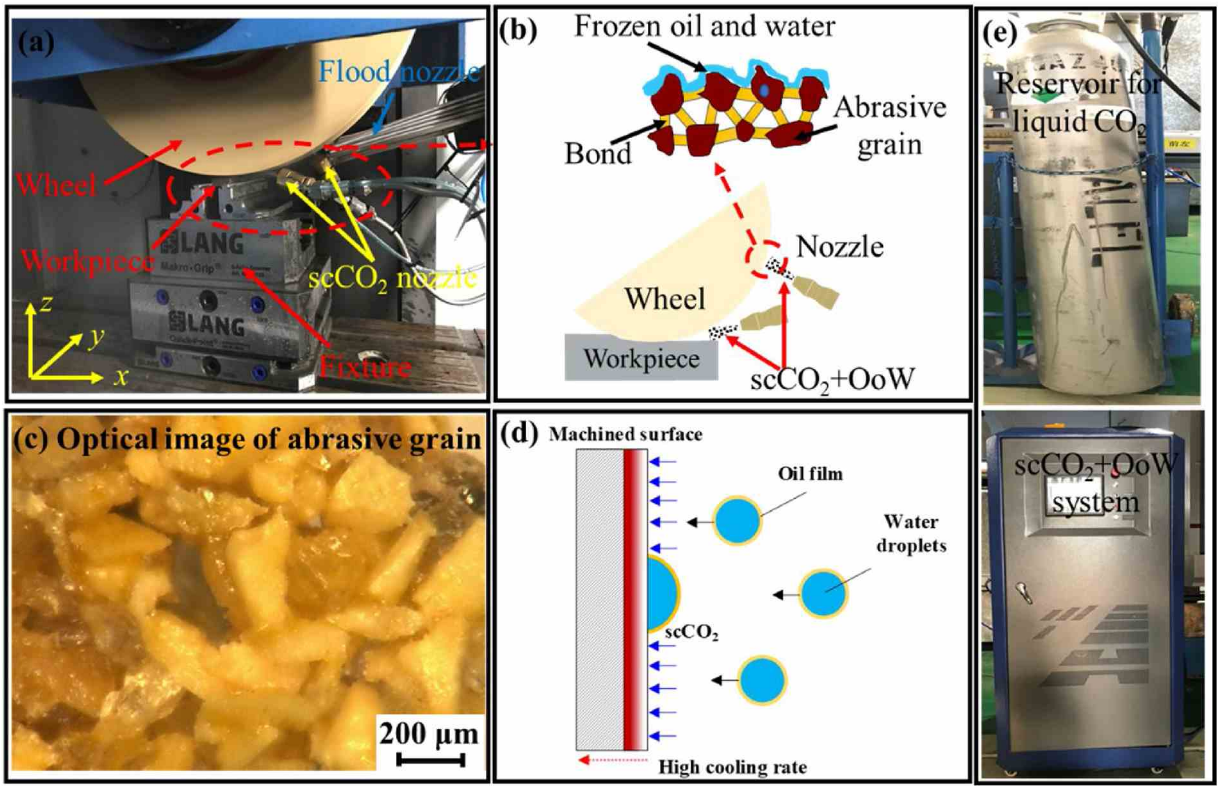

Fig. 3. (a) Experimental setup, (b) wheel-workpiece contact zone, (c) abrasive grain, (d) oil on water mechanism and (e) cooling system in the present work.

Table 4
Experimental grinding parameters.

Parameters	Description
Grinder	MKL 7132
Grinding wheel	P 400 × 50 × 127 ZA 60 H V
Wheel speed (v_s)	20 m/s
Feed rate (v_w)	100 mm/min
Depth of cut (a_p)	0.025, 0.050, 0.075 0.100 mm
Workpiece	300 M steel
Dresser	Diamond wheel
Dressing depth	0.2 mm
Dressing speed	Rough dressing: 600 mm/min; Finish dressing: 200 mm/min

keep the grains sharp and the speeds for rough and finish dressing are 600 mm/min and 300 mm/min, respectively.

Characterization

The change of surface topography with different cooling conditions was inspected by a laser scanning confocal microscope (LSCM) (Keyence VK-X200 Series) and SEM (Vega LaB6). The surface roughness was measured by a portable measuring instrument (Mitutoyo SJ-210). To analyze the microstructure of the superficial layer, images were gained by an OM (Keyence VHX-500 F) and high-resolution SEM (TESCAN MIRA3), which also provide EBSD analysis. Furthermore, in order to reveal the mechanism of microstructure alternation of top surface layer, transmission electron microscopy (TEM) was used in a Talos F200X G2 with a 200 KV acceleration voltage. The TEM specimen was prepared by focused Ion beam (FIB) method in a GAIA 3 machine with a thickness of about 40 nm. The microhardness of surface layer was detected by a TI 950 Triboindenter with the vibration polishing samples and the surface residual stresses of two orthogonal directions (X: grinding direction, Y: normal direction) was measured by a Proto LXRD system with Cr-Kα radiation source.

Results and discussion

Effect of cooling conditions on the surface morphology generation

The 3D topographies of the ground surface under the investigated cooling conditions are plotted in Fig. 4. By example of dry surface grinding, strong peaks and valleys are obviously shown on the surface morphology. When the fluid in flood form was introduced, the ground surface shows an improvement in terms of its surface finish. As the $scCO_2$ medium was applied for the grinding process, the maximum height difference (denoted as Δh_{max}) of surface profile sharply reduced and the machined surface shows smooth features. Interestingly, the generated surface with the hybrid cooling condition of $scCO_2$ and OoW seems not to be as better as those with single cryogenic medium. Obvious residual material that should be normally removed by the abrasives appeared on the machined surface instead. If the lubrication effect of the vegetable oil film was taken considered, the friction between abrasive edge and workpiece and therefore the cutting heat greatly reduced. Nevertheless, the exposed water on the wheel and workpiece surfaces can increase the possibility of regional wheel clogging in view of the chips and the cutting edges of abrasives will become blunt, both of which results in the residual material on the surface. This phenomenon will also be discussed in combination of the chip morphology change.

It is known that the ground surface is created by the superposition of scratches between numerous abrasives and workpiece. Therefore, the theoretical analysis of grinding depth of the single grit can be useful to compare the surface generation under different cooling conditions. As reported by Chuang et al. [26], the maximum undeformed chip thickness of the single grit can be described as:

$$h_m = 1.26 \times \left[\frac{\pi d^3 \tan\gamma}{6 f_a} \left(\frac{v_w}{v_s} \right) \sqrt{\frac{a}{D}} \right]^{1/3} \tag{1}$$

Where h_m is the maximum undeformed chip thickness, d is the grain size,

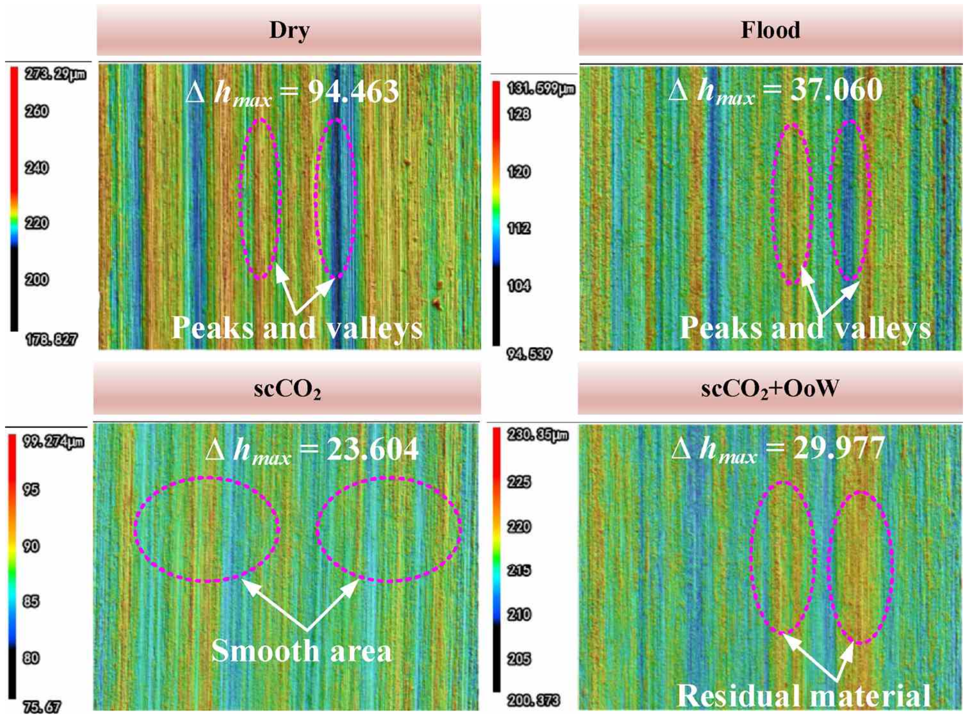

Fig. 4. 3D images of the ground surface with a constant grinding depth of 0.005 mm.

γ is half of the tip angle, f_a is the volume fraction of abrasives, v_w and v_s represent the workpiece feed and wheel speed, respectively, a is the grinding depth and D is the wheel diameter. It can be noted that the increase of grinding depth contributes to higher chip thickness. In other words, the number of grains for cutting operation per unit time increases and the accordance of notches of the surface profile which was finally created by the grit cutting theoretically presents improvement. In this case, the effect of cooling technique was enhanced as the grinding depth increases.

To reveal the effect of supplementary medium on the surface grinding performance, the recorded maximum height difference of surface profile with different cooling conditions as function of grinding depths is plotted in Fig. 5. Note that unstable change due to severe plastic flow of material occurred which is especially enlarged with grinding depth of 0.05 mm under dry condition while there exists a downtrend for the flood case as the grinding depth increases. It indicates

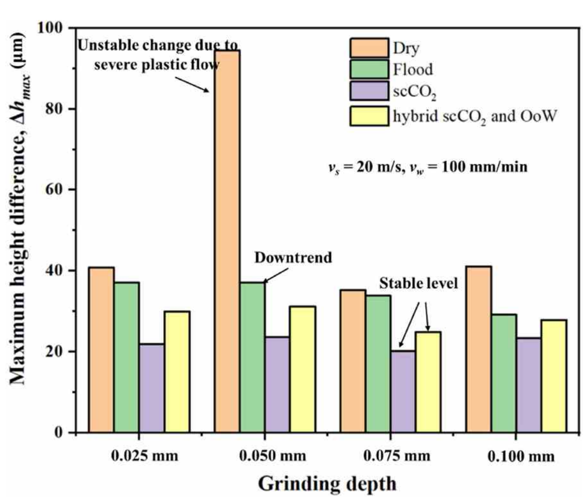

Fig. 5. Maximum height difference of surface profile with different cooling conditions.

stable levels for both $scCO_2$ and hybrid techniques being maintained at a lower level compared to dry and flood forms. This shows to increase the productivity and process sustainability, the $scCO_2$-based cooling conditions seem to be a better and feasible choice.

Fig. 6 shows a series of SEM images captured from the machined surfaces with different grinding depths and cooling conditions. It can be noted from Fig. 6 (a) that with dry condition high plastic flow of workpiece material on the surface occurred. As the grinding depth increases up to 0.1 mm, the generated workpiece surface presents lower plastic deformation compared to that of lower depth while some cavities due to the weld and breakage of abrasives appeared concerning the high generated heat as depicted in Fig. 6 (b). Meanwhile, the matched chips with the identical grinding parameters of Fig. 6 (b), (d), (f) and (h) are illustrated in Fig. 7 (a), (b), (c) and (d), respectively. Note that continuous ribbon chips were the outcome of dry surface grinding and serrated features were observed on the free surface of microchips. When the fluid in flood form was used, the ground surface quality shows an improvement, as plotted in Fig. 6 (c). The plastic flow shows weaker trace instead on the surface with regard to flood condition as the grinding depth becomes higher, as shown in Fig. 6 (d). This indicates the feasibility of improving the machining efficiency *via* parameter control when the 300 M steel was processed under flood grinding. In view of its chip morphology, the spherical and cracked chips are the case for flood surface grinding while the generated chips were easily taken away by the funning fluid (see Fig. 7 (b)). When the proposed $scCO_2$ medium was applied, the final created surfaces have been shown fully smooth features especially for the case of higher grinding depths which outlines unique advantages of $scCO_2$ medium for increased material removal rate (MRR), as depicted in Fig. 6 (e) and (f). From the matched chip morphology shown in Fig. 7 (c), it was found that the generated chips with $scCO_2$ condition was similar to that of dry condition. However, adhesion and sliding trace occasionally appeared on the surface when the mixture of $scCO_2$ and OoW was applied to the processing with smaller grinding depth, as shown in Fig. 6 (g) and it becomes regional deposition as the grinding depth increases, as shown in Fig. 6 (h). This can be attributed to the chip evolution from even ribbons to uneven spherical and fragmented chips as the Oow medium was added for the